

Faculty of Engineering
Faculty of Engineering - Papers

University of Wollongong

Year 2004

Characterization of Nanocrystalline
Si-MCMB Composite Anode Materials

G. X. Wang* J. Yao†

H. K. Liu‡

*University of Wollongong, gwang@uow.edu.au

†University of Wollongong, jyao@uow.edu.au

‡University of Wollongong, hua@uow.edu.au

This article was originally published as Wang, GX, Yao, J and Liu, HK, Characterization of Nanocrystalline Si-MCMB Composite Anode Materials, *Electrochemical and Solid-State Letters*, 7(8), 2004, A250-A253. Copyright The Electrochemical Society. Original journal available here.

This paper is posted at Research Online.

<http://ro.uow.edu.au/engpapers/139>



Characterization of Nanocrystalline Si-MCMB Composite Anode Materials

G. X. Wang,^z Jane Yao, and H. K. Liu*

Institute for Superconducting and Electronic Materials, University of Wollongong, New South Wales 2522, Australia

Nanocrystalline Si-mesocarbon microbeads (MCMB) composite anode materials were prepared by ballmilling. Scanning electron microscopic observation showed that the spherical shape of MCMB particles can be retained via moderate ballmilling. Ballmilling conditions have an impact on the capacity and cyclability of nanocrystalline Si-MCMB composites. The optimized Si-MCMB composite anode demonstrated a reversible capacity of 1066 mAh/g with good cyclability. A reaction model has been proposed to explain the reaction mechanisms of lithium insertion and extraction in the Si-MCMB electrode.
© 2004 The Electrochemical Society. [DOI: 10.1149/1.1764411] All rights reserved.

Manuscript submitted November 3, 2003; revised manuscript received December 21, 2003. Available electronically June 14, 2004.

Various types of carbonaceous materials such as natural and synthetic graphites, cokes, carbon and graphite fibers, pyrolysis carbons, and mesocarbon microbeads (MCMB), have been widely used as anode materials for lithium-ion batteries.¹⁻³ Carbon anodes have a theoretical lithium intercalation capacity of 372 mAh/g to form LiC_6 intercalation compound. Among them, mesocarbon microbeads (MCMB) represent an industry benchmark as anode materials for lithium-ion batteries, which deliver a reversible capacity of 300-340 mAh/g and excellent cyclability. Recently, various tin-based lithium storage alloys and tin oxide composites have attracted intensive investigation worldwide. The formation of $\text{Li}_{4.4}\text{Sn}$ results in a theoretical capacity of 991 mAh/g for element Sn. However, this alloying process is accompanied by a 259% volume increase, causing severe disintegration of the electrode (cracking and crumbling).^{4,5} This problem can be partly alleviated by using intermetallic tin alloys (M_xSn) such as Cu_6Sn_5 ,^{6,7} SnMnC ,⁸ FeSn_2 ,⁹⁻¹¹ Ni_3Sn_4 ,¹² and tin-based amorphous composite oxides (TCO).^{13,14} When M_xSn alloys react with lithium, Li_xSn alloys are formed. The inactive M matrixes are generated simultaneously, which are usually nanosize in nature and can buffer the volume increase of Li_xSn alloys. However, the cycle life for these tin alloys is still poor, preventing any practical application. Silicon has a high theoretical lithium storage capacity of 4000 mAh/g when forming $\text{Li}_{21}\text{Si}_5$ alloys. Wilson and Dahn¹⁵ have synthesized nanodispersed silicon in carbon using chemical vapor deposition (CVD). Although the Si-C anodes demonstrated a reversible capacity of 500 mAh/g, it is difficult to control the morphology of Si and C using the CVD approach. Niu and Lee¹⁶ dispersed crystalline silicon (325 mesh) in a sol-gel graphite matrix by ballmilling and achieved a reversible capacity of 832.2 mAh/g in the first cycle. Nano-Si-carbon composites have been prepared by hand mixing nano-Si and carbon black, which demonstrated a high reversible capacity of 1700 mAh/g.¹⁷ The lithium storage properties of nanostructured Si and Si film have also been investigated.^{18,19}

Since MCMB anode materials have the best cyclability among all the various types of carbon anode materials, the combination of MCMB and Si may result in Si-MCMB composite anode materials with high capacity and satisfactory rechargeability. Based on this hypothesis, we prepared nanocrystalline Si-MCMB composite materials by high-energy ballmilling. Their electrochemical properties as anodes in lithium-ion cells were systematically evaluated.

Experimental

Nanocrystalline Si with an average particle size of 80 nm was obtained from Nanostructured & Amorphous Materials Inc., USA, which were prepared by laser driven silane gas reaction. MCMB (MCMB-10 graphitizing) was supplied by Osaka Gas Co. (Japan). MCMB powders have an average particle size of 10 μm . Nanocryst-

talline Si-MCMB composites were prepared by high-energy ballmilling using a planetary ballmilling machine (Labtechnics, Australia). The nanocrystalline Si content in the composite is 20 wt %. We chose this percentage based on the results of a previous investigation on ballmilled Sn-graphite²⁰ and ballmilled Si-graphite.²¹ The mixtures were ballmilled for 5, 10, and 20 h, respectively, to obtain three batches of Si-MCMB composites. The as-prepared Si-MCMB composites were characterized by scanning electron microscopy (SEM, Leica/Cambridge Stereoscan 440 scanning electron microscope) and X-ray diffraction (XRD) with $\text{Cu K}\alpha$ radiation (MO3xHF22, MacScience, Japan).

The electrochemical properties of Si-MCMB composites were measured via coin cell testing. The Si-MCMB electrodes were made by dispersing 84 wt % active materials, 8 wt % carbon black, and 8 wt % polyvinylidene fluoride (PVDF) binder in dimethyl phthalate solvent to form a homogeneous slurry. The slurry was spread onto a copper foil. The coated electrodes were dried in a vacuum oven at 120°C for 12 h and then pressed to enhance the contact between the active materials and the conductive carbons. The CR2032 coin cells were assembled in an argon-filled glove box (Mbraun, Unilab, Germany) using lithium metal foil as the counter electrode. The electrolyte was 1 M LiPF_6 in a mixture of ethylene carbonate (EC) and dimethyl carbonate (DMC) (1:1 by volume, provided by Merck KgaA, Germany). The cells were galvanostatically discharged and charged in the range of 0.01-3 V at a current density of 0.05 mA/cm². Cyclic voltammetry (CV) was performed on a potentiostat (model M362, EG&G Princeton Applied Research, USA) at a scanning rate of 0.1 mV/s.

Results and Discussion

MCMB particles have a spherical shape. Figure 1a shows an SEM photo of MCMB particles, which consists of many small

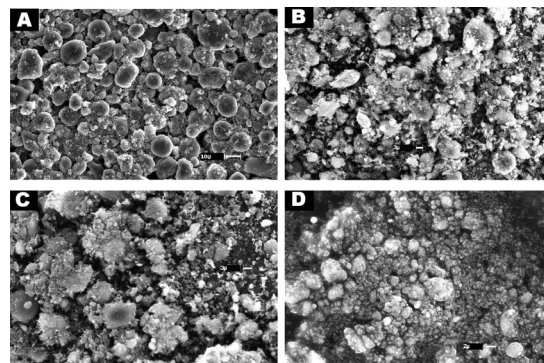


Figure 1. SEM image of (a) bare MCMB graphite, (b) 20 wt % nano Si-MCMB ballmilled for 5 h, (c) 20 wt % nano-Si-MCMB ballmilled for 10 h, and (d) 20 wt % nano-Si-MCMB ballmilled for 20 h.

* Electrochemical Society Active Member.

^z E-mail: gwang@uow.edu.au

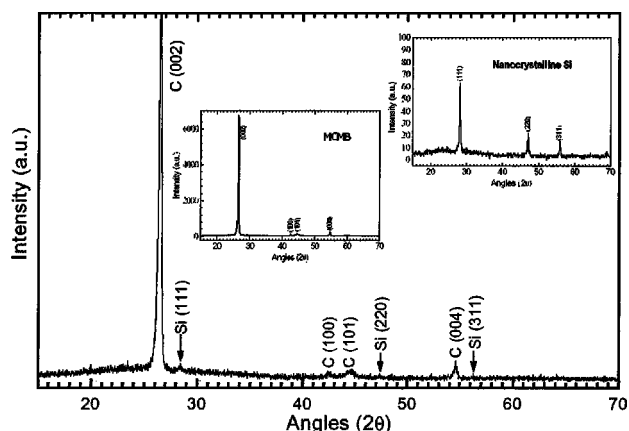


Figure 2. XRD pattern of 20 wt % nano-Si-MCMB ballmilled for 10 h.

graphite particles. The images of the Si-MCMB composites ballmilled for different times are shown in Fig. 1b, c, and d. After ballmilling for 5 and 10 h, the spherical agglomerates were partially broken. But most particles still retained a spherical shape. However, after 20 h extensive ballmilling, most spherical MCMB agglomerates were destroyed and formed finely ground graphite debris. Energy-dispersive spectrometry (EDS) detection was performed on the bulk of Si-MCMB composites and confirmed the presence of Si. Figure 2 shows the XRD pattern of Si-MCMB. As a comparison, the XRD patterns of bare MCMB and nanocrystalline Si are also presented in the inset. The intensities of the diffraction lines of nanocrystalline Si are much weaker than for MCMB graphite, indicating the nanocrystalline nature of Si. The ballmilling process caused slight broadening of the (002) peak of MCMB graphite. The full

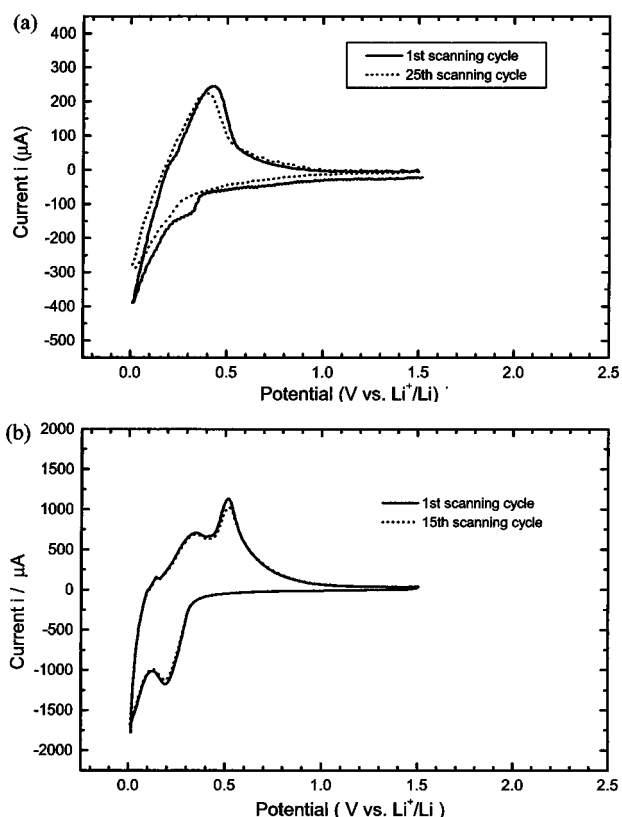


Figure 3. CVs of (a) MCMB electrode and (b) nano-Si-MCMB electrode (sample E).

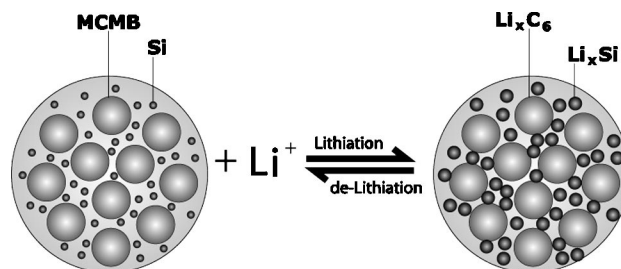


Figure 4. Schematic model of the lithiation and delithiation process in Si-MCMB composites. The volume increases due to the formation of Li_xSi alloys are small in local domain and effectively buffered by MCMB matrix.

width at half-maximum (fwhm) of (002) diffraction peak of MCMB were calculated to be 0.248, 0.250, 0.278, and 0.296° for pristine MCMB and 5 h ballmilled Si-MCMB, 10 h ballmilled Si-MCMB, and 20 h ballmilled Si-MCMB, respectively. No SiC phase was detected by XRD. Therefore, the mechanically added nanocrystalline Si forms Si-MCMB composites.

Cyclic voltammograms (CVs) of MCMB and Si-MCMB electrodes in lithium-ion cells, in which a lithium foil was used as the counter electrode and reference electrode, are shown in Fig. 3a and b, respectively. In Fig. 3a, the potential of the lithium ion insertion peak in the cyclic voltammetric curve of MCMB electrode is very close to 0.0 V vs. the Li/Li^+ reference electrode, whereas the potential of lithium extraction is in the range 0.3-0.4 V vs. the Li/Li^+ reference electrode. In Fig. 3b, one pair of additional reduction and oxidation peaks appeared in the CV curve of the Si-MCMB electrode, which is located at around 0.2 and 0.51 V vs. the Li/Li^+ reference electrode. This pair of redox peaks should correspond to

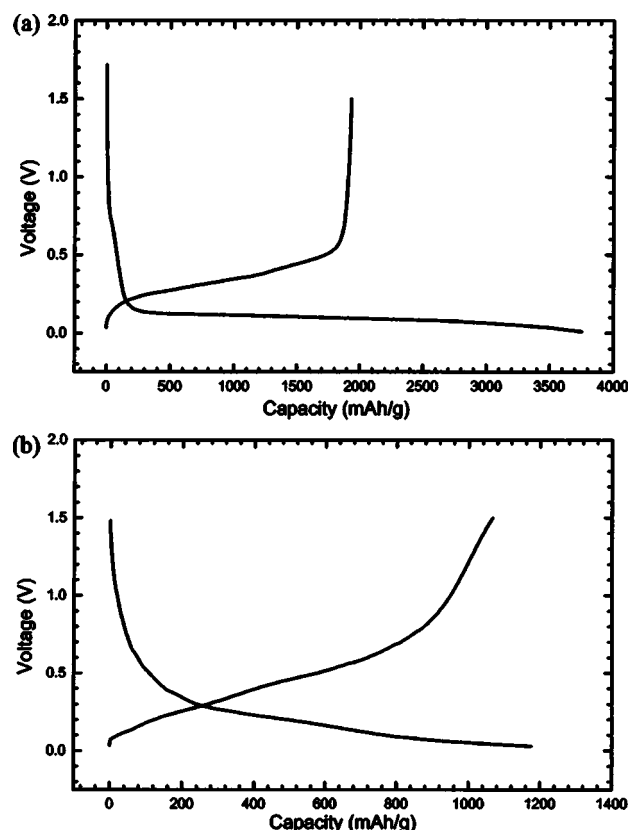


Figure 5. The discharge/charge profiles of (a) bare nano-Si electrode and (b) nano-Si-MCMB electrode (sample E).

Table I. Specific capacity in the first cycle for bare MCMB, bare nanocrystalline Si, and Si-MCMB electrodes.

Samples	$Q_{\text{discharge}}$ (mAh/g)	Q_{charge} (mAh/g)	$Q_{\text{irreversible}}$ (mAh/g)	Efficiency (%)
Sample A (bare MCMB)	355	325	25	91.5
Sample B (bare nanocrystalline Si)	3752	1931	1821	51.5
Sample C (20 wt % Si (2 μm) + MCMB, ballmilled for 10 h)	687	382	305	55.6
Sample D (20 wt % Si (nanocrystalline) + MCMB, ballmilled for 5 h)	1105	936	239	84.7
Sample E (20 wt % Si (nanocrystalline) + MCMB, ballmilled for 10 h)	1175	1066	115	90.7
Sample F (20 wt % Si (nanocrystalline) + MCMB, ballmilled for 20 h)	1273	1012	261	79.5

the lithiation and delithiation of Si in the MCMB matrix. The results of CV measurements clearly demonstrated that Si participated in the reaction with lithium ions.

The specific capacity and cyclability of nanocrystalline Si-MCMB composite electrodes were measured by constant current charge/discharge testing. Table I shows the discharge and charge capacities in the first cycle for different sample electrodes. The bare MCMB electrode (sample A) delivered a reversible capacity of 325 mAh/g in the first cycle with high efficiency. The bare nanocrystalline Si electrode (sample B) delivered a very high lithium storage capacity of 3752 mAh/g, which is very close to its theoretical capacity of 4000 mAh/g. However, this nanocrystalline Si anode had a very high irreversible capacity of about 1821 mAh/g in the first cycle. The formation of $\text{Li}_{1.2}\text{Si}$ alloys induces a 323% volume increase.⁴ Such high volume increase could create microcracks and therefore destroy the integrity of the electrode, causing high irreversible capacity and poor cyclability. Sample C is crystalline Si (2 μm)-MCMB composite prepared by ballmilling for 10 h. Sample C anode shows a lower specific capacity and poorer rechargeability than for nanocrystalline Si-MCMB electrodes (samples D, E, and F). The chemical reactivity of coarse crystalline Si is much lower than that of nanocrystalline Si. Correspondingly, the contribution to lithium storage capacity from Si is smaller. Because of the effect of the coarse particle size, the volume change in local domains in sample C anode may be much larger than for nanocrystalline Si when embedded in MCMB. Therefore, sample C demonstrates lower specific capacity and higher irreversible capacity on cycling.

The ballmilling time had a significant impact on the specific capacity and rechargeability of Si-MCMB composite anodes.

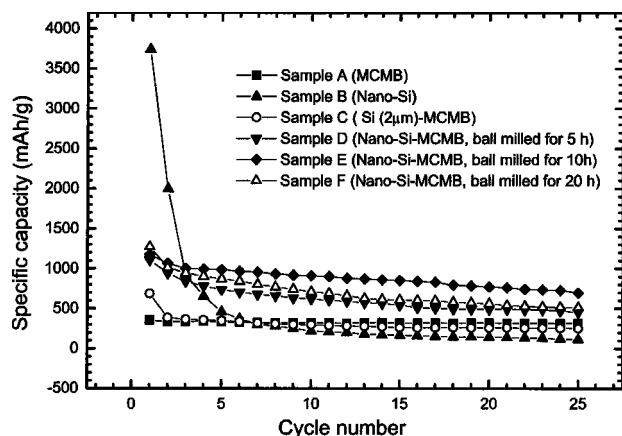


Figure 6. The discharge capacity vs. cycle number. Current density 0.05 mA cm^{-2} .

Sample E (ballmilled for 10 h) showed an optimal lithium storage capacity and capacity retention on cycling. We intended to use the ballmilling process to disperse nanocrystalline Si in MCMB matrix. The longer the ballmilling time, the better the dispersing effect that is obtained. However, ballmilling inevitably breaks up the MCMB spherical particles and destroys the graphite structure, therefore degrading the electrochemical properties of MCMB electrodes. Long-time ballmilling induces high surface area of MCMB powders. The irreversible capacity in the first cycle is considered coming from the formation of a passivating film, which consumes lithium at the electrode materials/electrolyte interface.²¹⁻²³ From SEM observation, we found that the spherical MCMB particles were severely damaged after 20 h ballmilling. Therefore, the sample F (ballmilled for 20 h) anode exhibited a very high irreversible capacity. To achieve better electrochemical performance for nanocrystalline Si-MCMB anodes, Si must be dispersed homogeneously in the MCMB matrix without damaging the spherical MCMB structure. Sample E seems to meet this requirement.

To combat the problems caused by volume increase in the alloying process, reducing the particle size of Si is an efficient way to minimize the volume change in local domains due to the formation of Li_xSi alloys. Another approach to overcome this issue is to embed the active element in an inactive matrix to let the inactive matrix absorb or buffer the volume expansion. The intermetallic MM' alloys and tin composite oxides (TCO) are exactly designed to utilize this principle. We embedded nanocrystalline Si particles in an MCMB matrix through moderate ballmilling. When lithium ions are inserted into Si-MCMB composites, nano-Si reacts with Li to form Li_xSi alloys and MCMB graphite reacts with Li to form Li_xC_6 . The intercalation of Li in MCMB graphite causes only minor changes of interlayer spacing and stacking order. MCMB graphite is almost dimensionally invariable during lithium insertion and extraction.²⁴ Because Si particles are nanosize in nature, the volume increase in the local environment is small, and can be easily absorbed by the ductile MCMB graphite matrix surrounded around nano-Si clusters. As a result, the volume change in the macrodomain is small and negligible for Si-MCMB electrodes. During the lithium extraction process, a similar phenomena occurs. This allows the integrity of the electrode to be preserved for repeated lithium insertion and extraction. A schematic model of the lithiation and delithiation process in Si-MCMB composite was proposed and presented in Fig. 4.

Figure 5 shows the discharge/charge profiles in the first cycle for bare nanocrystalline Si (sample B) and nano-Si-MCMB (sample E) anodes. The nanocrystalline Si electrode shows a flat discharge plateau between 0.2 and 0.05 V, corresponding to the reduction peak in the CV curve (Fig. 3b), indicating the highly reactive nature of nanocrystalline Si powders. In contrast, the Si-MCMB (sample E) anode shows a parabolic curve between 0.5 and 0.2 V and a flat plateau between 0.1 and 0.0 V, which is typical for composite electrode materials. The cyclabilities of all the sample anodes are shown

in Fig. 6. The bare MCMB anode is very stable on cycling, but with limited capacity. Although the bare nanocrystalline Si anode (sample B) has a high initial capacity, its capacity decreased quickly on cycling. Therefore, it is not suitable to use nanocrystalline Si alone as an electrode in Li-ion cells. Generally, nanocrystalline Si-MCMB composite electrodes demonstrated superior performance (high capacity and satisfactory cyclability), compared to bare MCMB and bare nano-Si electrodes. In particular, sample E shows stable cyclability similar to the bare MCMB electrode, but with much higher capacity. We believe that the electrochemical performance of nano-Si-MCMB composites may be further optimized through tuning the material processing.

Conclusions

Nanocrystalline Si-MCMB composite anode materials were prepared by ballmilling. They are intended to utilize the high capacity of Si and the stable cyclability of MCMB. The CV measurements show that Si participates in the reaction with lithium in Li-ion cells. In this investigation, we achieved a reversible capacity of 1066 mAh/g for nanocrystalline Si-MCMB composites and fairly good cyclability. A reaction model was proposed for the lithiation and delithiation process in the Si-MCMB electrodes in lithium-ion cells.

Acknowledgments

The authors express their thanks for financial support from the Australia Research Council through ARC Linkage project (LP0219309) with industry partner, Sons of Gwalia Ltd. We thank Professor J. Y. Lee for fruitful discussion.

The University of Wollongong assisted in meeting the publication costs of this article.

References

1. D. Guymard and J. M. Tarascon, *J. Electrochem. Soc.*, **139**, 937 (1992).
2. K. Sato, M. Noguchi, A. Demachi, N. Oki, and M. Endo, *Science*, **264**, 556 (1994).
3. J. R. Dahn, T. Zheng, Y. H. Liu, and J. S. Xue, *Science*, **270**, 590 (1995).
4. M. Winter and J. O. Besenhard, *Electrochim. Acta*, **45**, 31 (1999).
5. D. Fauteux, *J. Appl. Electrochem.*, **23**, 1 (1993).
6. K. D. Kepler, J. T. Vaughey, and M. M. Thackeray, *Electrochem. Solid-State Lett.*, **2**, 307 (1999).
7. G. X. Wang, L. Sun, D. H. Bradhurst, S. X. Dou, and H. K. Liu, *J. Alloys Compd.*, **147**, 3237 (2000).
8. L. Y. Beaulieu and J. R. Dahn, *J. Electrochem. Soc.*, **147**, 3237 (2000).
9. O. Mao, R. L. Turner, L. A. Courtney, B. D. Fredericksen, M. J. Buckett, L. J. Krause, and J. R. Dahn, *Electrochem. Solid-State Lett.*, **2**, 3 (1999).
10. O. Mao, R. A. Dunlap, and J. R. Dahn, *J. Electrochem. Soc.*, **146**, 405 (1999).
11. O. Mao and J. R. Dahn, *J. Electrochem. Soc.*, **146**, 414 (1999).
12. J.-H. Ahn, G. X. Wang, M. J. Lindsay, S. X. Dou, and H. K. Liu, *J. Metastable Nanocryst. Mater.*, **10**, 595 (2001).
13. Y. Idota, U.S. Pat. 5,478,671 (1995).
14. Y. Idota, T. Kubota, A. Matsufuji, Y. Maekawa, and T. Miyasaka, *Science*, **276**, 1395 (1997).
15. A. M. Wilson and J. R. Dahn, *J. Electrochem. Soc.*, **142**, 326 (1995).
16. J. Niu and J. Y. Lee, *Electrochem. Solid-State Lett.*, **5**, A107 (2002).
17. H. Li, X. J. Huang, L. Q. Chen, Z. G. Wu, and Y. Liang, *Electrochem. Solid-State Lett.*, **2**, 547 (1999).
18. J. Graetz, C. C. Ahn, R. Yazami, and B. Fultz, *Electrochem. Solid-State Lett.*, **6**, A194 (2003).
19. S. Ohara, J. Suzuki, K. Sekine, and T. Takamura, *J. Power Sources*, **119-121**, 591 (2003).
20. G. X. Wang, M. J. Lindsay, L. Sun, D. H. Bradhurst, S. X. Dou, and H. K. Liu, *J. Power Sources*, **97-98**, 211 (2001).
21. C. S. Wang, G. T. Wu, X. B. Zhang, Z. F. Qi, and W. Z. Li, *J. Electrochem. Soc.*, **145**, 2751 (1998).
22. F. Disma, L. Aymard, L. Dupont, and J.-M. Tarascon, *J. Electrochem. Soc.*, **143**, 3959 (1996).
23. F. Disma, C. Lenain, B. Beaudoin, L. Aymard, and J.-M. Tarascon, *Solid State Ionics*, **98**, 145 (1997).
24. J. O. Besenhard, J. Yang, and M. Winter, *J. Power Sources*, **68**, 87 (1997).